

# Histological assessment of tissue from large human bone defects repaired with $\beta$ -tricalcium phosphate

Tomas Kucera · Pavel Sponer · Karel Urban · Ales Kohout

Received: 13 August 2013 / Accepted: 24 September 2013 / Published online: 5 October 2013  
© Springer-Verlag France 2013

**Abstract** This report describes the histological characteristics of large human bone defects that were implanted with  $\beta$ -tricalcium phosphate ( $\beta$ -TCP). Samples were obtained longer after the primary operation than in the earlier studies. We assessed a total of nine biopsies taken 33–208 weeks after implantation. The tissue sections were stained with hematoxylin–eosin for general observation, with Gomori stain to visualize the reticulin fibers, and with an antibody against tartrate-resistant alkaline phosphatase (TRAP) to characterize the cells. Ongoing bone remodeling was observed even 208 weeks after implantation as determined by the presence of osteoclasts and active osteoblasts and new woven and lamellar bone. We observed multinuclear giant cells phagocytosing the biomaterial and the attachment of osteoclasts to the  $\beta$ -TCP. The osteoclasts showed intense TRAP positivity, while the giant cells showed variable TRAP positivity. There was a zonal pattern in the original defects: The central regions showed granules and fibrous septa, while peripheral areas showed a layer of new bone formation. These data demonstrate ongoing bone remodeling long after implantation in the peripheral regions of the original defects as well as fibrous

changes in the central regions and phagocytosis of biomaterial by multinuclear giant cells.

**Keywords** Foreign body reactions (response) · Bone remodeling · Calcium phosphate(s)

## Introduction

A variety of biomaterials, including bioceramics, biopolymers, metals, and composites, have been used to fill bone defects. Numerous studies have demonstrated that porous calcium phosphate bioceramics are very useful as synthetic biomaterials due to their excellent biocompatibility and their ability to bond to living bone. Hydroxyapatite,  $\beta$ -tricalcium phosphate ( $\beta$ -TCP), and their derivatives, alone or in combination, are the most commonly used ceramic materials in the clinical setting because of their chemical similarity to the mineral makeup of human bones and teeth. Radiography shows the implanted  $\beta$ -TCP to be well incorporated into the surrounding bone with a resorption rate that is dependent on the defect size. Aside from the chemical composition, the microstructure (i.e., the volume, density, and size of pores and the interconnections and specific surface) also impacts the extent and rate of bone penetration. However, histological studies of  $\beta$ -TCP used in large human bone defects are limited. It is thought that the material is at least partially resorbed and replaced by newly formed bone around the implanted material early after implantation, while bone formation becomes inactive late after implantation.

The purpose of this study was to investigate the bone-forming process around this ceramic bone graft material by determining the histological characteristics of large bone defects filled with  $\beta$ -TCP in seven patients.

T. Kucera (✉) · P. Sponer · K. Urban  
Department of Orthopaedic Surgery, University Hospital,  
Sokolska 581, 500 05 Hradec Kralove, Czech Republic  
e-mail: kucerat@tiscali.cz

T. Kucera · P. Sponer · K. Urban · A. Kohout  
Faculty of Medicine in Hradec Kralove, Charles University  
in Prague, Prague, Czech Republic

A. Kohout  
Fingerland's Department of Pathology, University Hospital,  
Hradec Kralove, Czech Republic

## Materials and methods

### Biomaterial

We have used interconnected  $\beta$ -TCP to repair bone defects since 2002. This material (Poresorb-TCP<sup>®</sup>, Lasak Ltd., Prague, Czech Republic) has a porosity of  $35 \pm 5 \%$ , an average macropore size  $100 \mu\text{m}$  in diameter, an average micropore size of  $3 \pm 2 \mu\text{m}$ , and a  $1,180^\circ\text{C}$  sintering temperature. It comes in a granule form made up of  $1.3 \pm 0.7 \text{ mm}$  particles and is manufactured to extraordinarily high purity.

### Patients

We have treated some bone lesions by curettage and implantation of  $\beta$ -TCP in our department since 2002. The study group of  $\beta$ -TCP implant patients included 91 patients; of these, we harvested a tissue sample from the original region of the defect that was filled by ceramic biomaterial from seven patients. Five of seven patients were children. Three biopsies were taken for histological examination during repeated surgeries performed on one patient, and one biopsy was taken from each of the other six patients. Thus, we assessed a total of nine biopsies. The age of the patients at the time of surgery ranged from 7 to 60 years. The reasons for histological evaluation of the implanted bioceramics were as follows: removal of the osteosynthetic material (5), surgery for tumor recurrence (2), osteosynthesis of pathologic fracture in the previously filled defect (1), and additional wide excision (1). The project was approved by the Ethics Committee of our University Hospital.

### Sample preparation

The tissue specimens were fixed in 10 % neutral-buffered formalin, decalcified in 5 % formic acid, and embedded in paraffin. Paraffin sections ( $4 \mu\text{m}$ ) were used for the histological and immunohistochemical studies. For light microscopy, sections were stained with hematoxylin and eosin (HE), while Gomori stain was used to visualize the reticulin fibers.

The immunohistochemistry was performed using a Ventana BenchMark ULTRA Advanced Staining System (Ventana Medical Systems, Inc., USA) with the UltraView Universal DAB Detection Kit after heat-induced epitope retrieval at  $95^\circ\text{C}$  in cell-conditioning medium CC1 for 64 min. This was followed by a 32-minute incubation with primary antibody (mouse monoclonal CD68 antibody, clone PG-M1, DAKO, dilution 1:50) at  $37^\circ\text{C}$ . In addition, tissue sections were stained with antibody against tartrate-resistant alkaline phosphatase (TRAP). The tissue sections

were incubated for 10 min in the histoprocessor (for pH 6 pretreatment). The antibody (TRAP, Abcam, dilution 1:750) was incubated at room temperature for 30 min, and the reaction was visualized using the EnVision Peroxidase Kit (DAKO, Glostrup, Denmark).

## Results

Data for the clinical cases described in this report are summarized in Table 1.

Case 1 (47-year-old female; biopsy taken 33 weeks after implantation)

The preoperative (CT scan imaging) and intraoperative (frozen section) diagnosis of this patient was a benign bone tumor of the distal femur. The patient underwent curettage and  $\beta$ -TCP filling. Two weeks later, a revision operation was performed due to restricted motion of the knee, pain, and synovitis. The intraoperative finding was leak of the  $\beta$ -TCP particles into the joint space. The final histological diagnosis was low-grade chondrosarcoma (grade I); 33 weeks after the first operation, wide resection and prosthetic replacement of the knee were performed. The entire femoral condyle with the original bone defect (size,  $25 \times 30 \text{ mm}$ ) was available for histological examination. A striking zonal pattern was present (Fig. 1). The central region comprised sheets of colorless birefringent granules of biomaterial separated by hypocellular fibrous septa. These septa sometimes contained small thin-walled blood vessels. The central region was surrounded by a zone of new bone formation around the biomaterial granules. Moreover, numerous foreign body multinuclear giant cells were associated with the  $\beta$ -TCP granules. No fibrosis or edema was observed in the surrounding bone; these were only seen proximal to the defect where widening of the bone trabeculae was associated with mildly sclerotic bone.

Case 2 (15-year-old male, biopsy taken 40 weeks after implantation)

The final diagnosis was recurrence of unicameral bone cyst on the proximal femur. The patient underwent curettage and grafting with a mixture of  $\beta$ -TCP and autogenous bone chips from the iliac crest. Additional metal plate osteosynthesis was performed. The osteosynthetic material was removed 40 weeks later, and tissue from the original defect was obtained at this time. Histologically, one half of the specimen was composed of nodular aggregates of empty spaces (where biomaterial was dissolved during tissue processing) that were separated by hypocellular fibrous septa. In the other half of the specimen, there was focal

**Table 1** Summary of clinical findings

Case no.	Age (years)	Sex	Final diagnosis	Location and tumor size	Amount of ceramic used (g)	Interval to biopsy (weeks)	Reason for surgery
1	47	F	Low-grade chondrosarcoma	Distal femur 40 × 40 × 40 mm	20	33	Wide resection
2	15	M	Recurrence of unicameral bone cyst	Proximal femur 140 × 35 × 30 mm	66 + autografts	40	Removal of osteosynthetic material
3	7	F	Fibrous dysplasia	Proximal femur 45 × 35 × 30 mm	14	50 53 106	Recurrence Fracture Removal of osteosynthetic material
4	60	F	Compression fracture	Proximal tibia 30 × 30 × 15 mm	12	53	Removal of osteosynthetic material
5	13	M	Nonossifying fibroma	Proximal tibia 40 × 30 × 20 mm	4	61	Removal of osteosynthetic material
6	17	M	Bone cyst in neurofibromatosis	Proximal tibia 85 × 125 × 30 mm	30	75	Removal of osteosynthetic material
7	11	M	Unicameral bone cyst	Proximal femur 44 × 27 × 25 mm	25	208	Recurrence

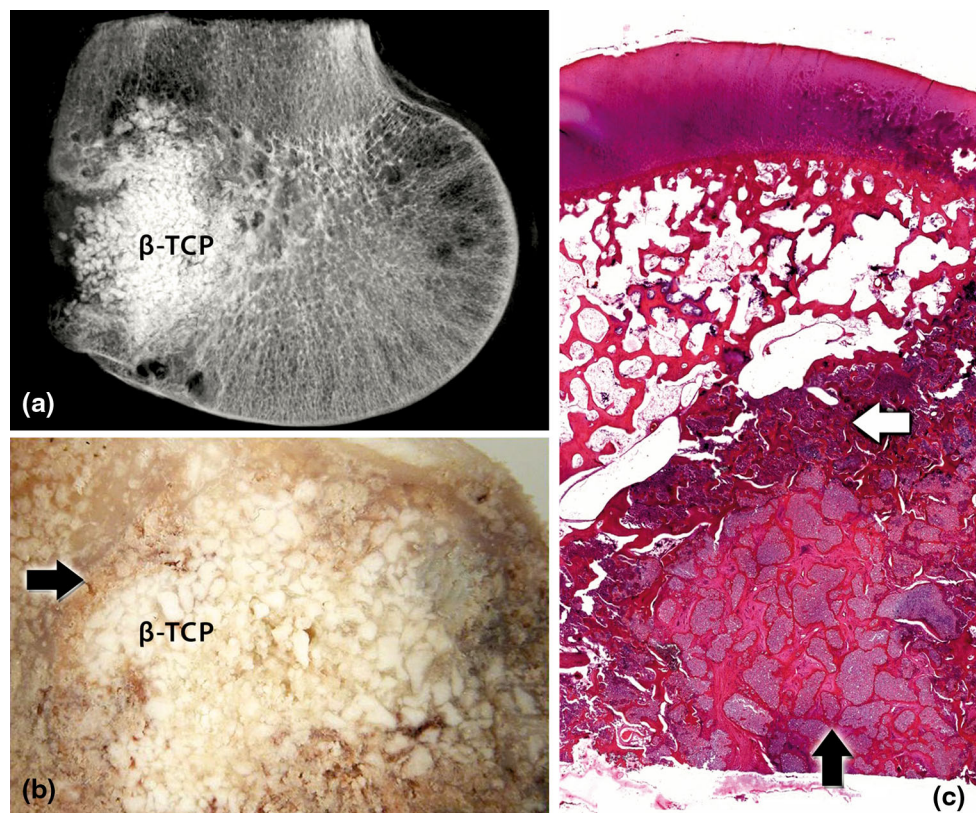


**Fig. 1** **a** A radiograph of the bone specimen from case 1: The entire femoral condyle is visible with the defect filled with  $\beta$ -TCP granules in direct contact with bone trabeculae after resection. **b** A macroscopic view of the specimen used for histological assessment. The central region was filled by  $\beta$ -TCP and surrounded by new bone

(arrow). **c** Histotopogram. HE staining. There was a zonal pattern of tissue reaction: The central region of the filled defect showed granules and fibrous septa (black arrow), while the peripheral region showed a layer of new bone formation (white arrow)

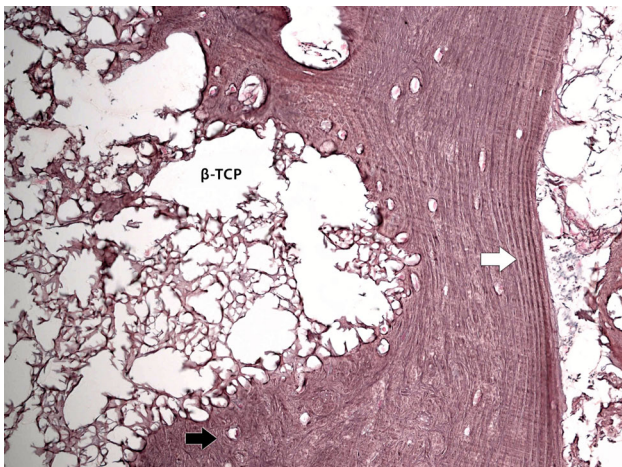


**Fig. 2** In this biopsy from case 2, the biomaterial is surrounded by new woven bone (*black arrow*) and lamellar bone (*white arrow*). The  $\beta$ -TCP was dissolved during the processing of the sample, and fibrous septa are visible in the central region Gomori staining; magnification  $\times 200$

formation of new woven and lamellar bone that was associated with the biomaterial (Fig. 2).

Case 3 (7-year-old female, biopsies taken 50, 53, and 106 weeks after implantation)

This patient suffered from fibrous dysplasia of the proximal femur. She underwent curettage and  $\beta$ -TCP implantation, and additional osteosynthesis with a plate was performed. Surgery due to recurrence was indicated 50 weeks later. The plate was removed and new curettage and  $\beta$ -TCP grafting was performed. Some tissue was removed and subjected to histological examination. Histological analysis showed sheets of biomaterial surrounded by foreign body multinuclear giant cells, foamy macrophages, and irregular foci of osteoid and woven bone. Three weeks later, the patient sustained a fracture of the proximal femur. Osteosynthesis was necessary with grafting using autogenous bone from the iliac crest. At this time, another tissue sample was acquired for histological examination. We observed necrotic tissue, fibrin, and granules of birefringent biomaterial. The plate was removed 53 weeks later (106 weeks after the first operation), and again a tissue sample was obtained from the original defect. We observed lamellar bone covered by periosteum. There were a few granules of biomaterial in the adjacent bone marrow.

Case 4 (60-year-old female, biopsy taken 53 weeks after implantation)

This patient sustained a fracture in the proximal region of the tibia. Osteosynthesis was performed with a metal plate and  $\beta$ -TCP implantation in the bone defect in the

metaphysis. The plate was removed 53 weeks later, and a sample of tissue from the original defect was obtained. Histological analysis showed granules of biomaterial with newly formed woven and lamellar bone on their surface. In addition, there were fragments of dense fibrous tissue that probably represented periosteum. Scattered chronic lymphocytic infiltrates and multinucleated giant cells were observed around the biomaterial.

Case 5 (13-year-old male, biopsy taken 61 weeks after implantation)

The final diagnosis was pathologic fracture of the proximal tibia at the focus of a fibrous cortical defect. A tissue sample was obtained when the osteosynthetic material was removed 61 weeks after the original surgery. Histological analysis showed irregular broad bone trabeculae. The intertrabecular space contained fibrous tissue with numerous foamy histiocytes and granules of biomaterial surrounded by multinucleated giant cells. Newly formed bone tissue was present in association with the biomaterial, which was focally entrapped within the trabeculae of new bone.

Case 6 (17-year-old male, biopsy taken 75 weeks after implantation)

The final diagnosis for case 6 was neurofibromatosis. Curettage,  $\beta$ -TCP grafting, and additional metal plate osteosynthesis of the cyst were performed in the tibia. The plate was removed 75 weeks later, and a sample of tissue was harvested at that time. Histological analysis showed trabeculae of the lamellar bone and fibrosis of the intertrabecular space. There were empty areas in which the biomaterial had been dissolved during sample processing. These spaces were surrounded by multinucleated giant cells, and the surface of some of these spaces showed foci of newly formed bone (Fig. 3). Cortical bone covered by periosteum was observed as well.

Case 7 (11-year-old male, biopsy taken 208 weeks after implantation)

This patient suffered from a unicameral bone cyst in the proximal femur. Curettage and  $\beta$ -TCP filling were performed, but surgery for cyst recurrence was indicated 208 weeks later. A tissue sample was obtained during the surgery. Histological analysis showed spongy bone, and there was an area measuring 6 mm in diameter that was composed of coarsely granular biomaterial. In the central region, the biomaterial was surrounded by fibrous tissue. In the periphery, focal new bone formation was seen in association with the biomaterial. In addition, scattered

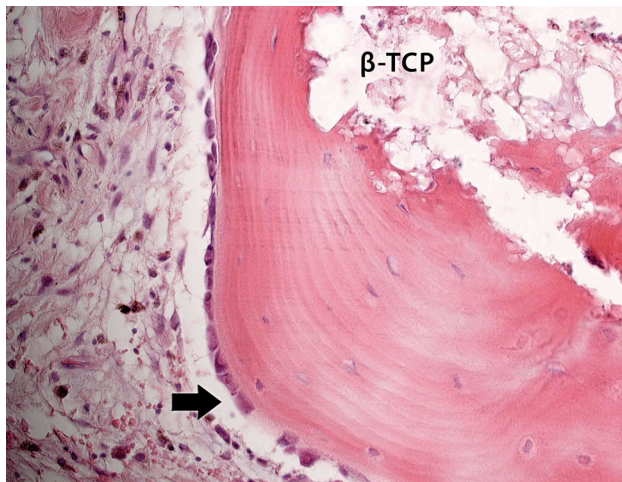


**Fig. 3** New bone formation around the biomaterial in the biopsy from case 6. Lamellar bone with osteocytes and a rim of active osteoblasts on the surface (*arrow*) can be seen. HE staining; magnification  $\times 200$

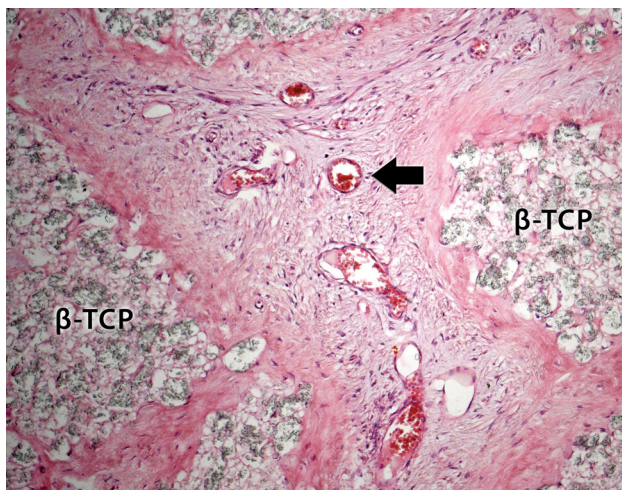


**Fig. 4** Fibrous septa containing blood vessels (*arrow*) among the  $\beta$ -TCP granules in the central region of the original defect in the biopsy from case 1. HE staining; magnification  $\times 200$

multinucleated giant cells were observed engulfing the biomaterial granules.

Notably, histological examination of all of the biopsies showed similar patterns. The central regions of the original defects were composed of granules of the  $\beta$ -TCP biomaterial separated by fibrous septa. These were not avascular zones; rather, some blood vessels were seen in these hypocellular tissues (Fig. 4).

Active new bone formation was observed in the peripheral regions of the original defects on the surface of the biomaterial. Woven and lamellar bone with osteoblasts and osteocytes was also seen (note the focal bone growth). Fig. 5 shows the new bone formation with osteoblasts and osteoclasts attached to the biomaterial. In contrast to the

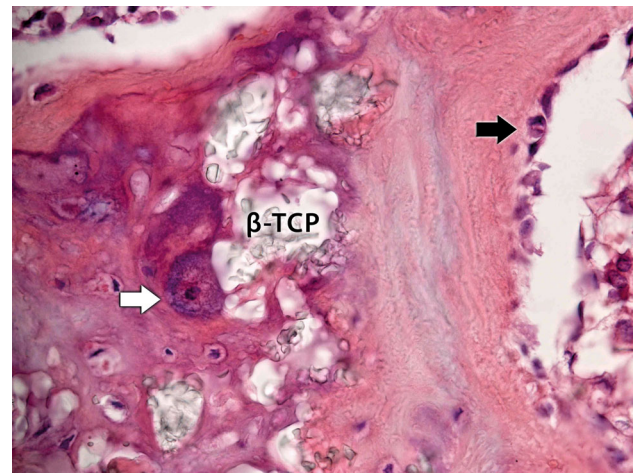


**Fig. 5** Biopsy from case 1. Active cell-based resorption was demonstrated by osteoclast attachment to the biomaterial (*white arrow*). Active bone remodeling was demonstrated by osteocytes within the new bone around the  $\beta$ -TCP and by active osteoblasts on the surface of lamellar new bone (*black arrow*). HE staining; magnification  $\times 400$

multinuclear giant cells, which were engulfing the biomaterial (Fig. 6), we did not observe osteoclasts engulfing the biomaterial.

All samples were examined for TRAP positivity. All biopsies showed that the osteoclasts and multinucleated giant cells in contact with the biomaterial expressed TRAP. In general, TRAP positivity was stronger in true osteoclasts and less intense and more heterogeneous in the giant cells, but occasionally TRAP expression in giant cells was as intense as in osteoclasts (Fig. 7). The foamy macrophages were TRAP negative. Three types of cells showed CD68 positivity: osteoclasts, multinucleated giant cells, and foamy macrophages.

## Discussion

$\beta$ -tricalcium phosphate is a widely used synthetic bone graft substitute [1], and its stoichiometry is similar to that of the amorphous precursors to bone mineral.  $\beta$ -TCP has excellent osteoconductive activity, and it is a porous resorbable biomaterial with the potential to be replaced by mature new bone. At present, there are many versions of  $\beta$ -TCP that differ in their porosity, shape, and size. Even though the chemical composition is the same, these other properties can influence the growth and proliferation of mesenchymal and endothelial cells and, consequently, affect the formation of new bone [2].

Bioresorption of  $\beta$ -TCP and concomitant bone formation has been demonstrated in animal studies that have included histologic assessment of bone samples [3–6]. A

limitation of these studies is the size of the experimental defects. The volume of the experimentally induced bone defects depends on the type of animal, but most defects are in the range of 0.1–3 cm<sup>3</sup> [7–9]. Furthermore, additional factors impact bone healing in experimental studies: the healing time may depend on the species and age of the animal, for example, and bone healing may be different in animals than in humans (e.g., the enchondral ossification that occurs in mice and rats) [10]. However, in human medicine, the bone defects are larger, often in the range of 0.4–173 cm<sup>3</sup> [11, 12], and the studies often focus on radiological evaluation of the healing of bone defects. There are just a few reports about the histological analysis of the healing of large bone defects filled with  $\beta$ -TCP in human bones [13–17]. In this study, we conducted a histological assessment of samples that were obtained longer after the primary operation than in the earlier studies. This enabled us to evaluate the healing process in the peripheral and central regions of the defect, to investigate the reaction

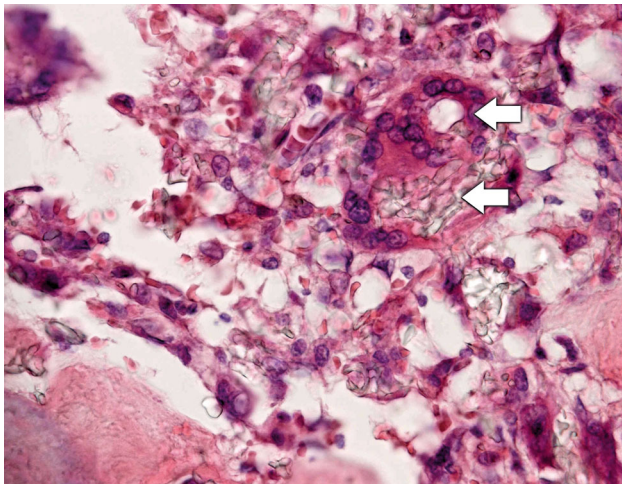


**Fig. 6** Biopsy from case 6. Multinucleated cells with engulfed biomaterial (*arrows*) were seen even 75 weeks after grafting. HE staining; magnification  $\times 400$

of the host tissue to the graft, and to look for signs of angiogenesis.

We observed direct new bone formation and bonding to  $\beta$ -TCP in the biopsies we examined. Most of the surface of the  $\beta$ -TCP in all of the samples was covered with immature woven and lamellar bone. Surprisingly, osteoblasts and osteocytes were present even 208 weeks (over 4 years) after grafting. There was no inflammatory reaction around the  $\beta$ -TCP particles, and we did not observe fibrous capsules forming around the  $\beta$ -TCP either. These findings demonstrated the satisfactory biocompatibility of this biomaterial. The reliable biocompatibility and osteoconductivity of  $\beta$ -TCP are due to its surface characteristics; importantly,  $\beta$ -TCP can absorb an appropriate spectrum of proteins and allows ion exchange to occur [18–21]. Two interesting findings of this study were that permanent bone formation occurred on the surface of  $\beta$ -TCP and that remodeling occurred 208 weeks after implantation. In addition, we observed the formation of new periosteum in some places.

$\beta$ -tricalcium phosphate is a resorbable bone graft substitute. Relatively little is known about the mechanism of resorption, but a combination of dissolution and enzymatic and phagocytic processes seems to be involved [22]. It is difficult to evaluate dissolution. The finding of empty spaces by microscopic examinations is rather due to dissolution of the  $\beta$ -TCP during sample preparation than to dissolution in vivo. We did observe giant cells and osteoclasts that seemed to be resorbing the biomaterial, but rather than engulfing the biomaterial, the osteoclasts may have been involved in enzymatic processes that contributed to resorption. One unanswered question remains: What role do osteoclasts play in remodeling the biomaterial once osteogenesis begins? One report suggests that osteoclasts remodel only the hydroxycarbonate apatite layer [23].

The role of the multinucleated giant cells remains unclear. Chazono et al. [4] observed these cells in resorptive lacunae in rabbit experiments. The appearance of

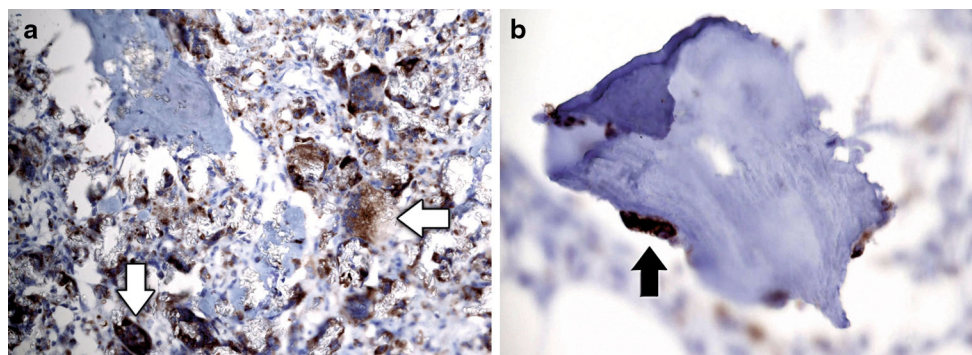


**Fig. 7 a** Biopsy from case 1. Giant cells showed variable TRAP positivity (*arrows*); these cells were larger and had many more nuclei than osteoclasts. TRAP staining; magnification,  $\times 200$ . **b** Biopsy from

case 4. Intense TRAP positivity in an osteoclast (*arrow*) localized to the lamellar bone surface. TRAP staining; magnification  $\times 400$

TRAP-positive multinucleated cells was followed by new bone formation, and the authors hypothesized that this indicated cell-based resorption of  $\beta$ -TCP. These results from animal experiments were confirmed by Ogose et al. [14] in humans early after  $\beta$ -TCP implantation.

It is difficult to distinguish between foreign body giant cells and osteoclasts by histologic examination. Ogose et al. used positive TRAP, CD68, and cathepsin K reactions to indicate the osteoclast-like nature of multinucleated giant cells in the tissue around the filling material. However, the foreign body giant cells were also positive for TRAP and CD68 [24, 25]. In this study, we observed numerous giant cells in the tissue surrounding the granules of  $\beta$ -TCP. We tried to distinguish between osteoclasts and foreign body multinuclear giant cells. Both types of cells expressed TRAP; notably, in true osteoclasts, the TRAP positivity was generally stronger. This is a rather nonspecific sign, however. It is possible to distinguish between osteoclasts and multinuclear giant cells on the basis of their structural characteristics. Multinucleated giant cells are larger and have more nuclei than osteoclasts (8–10 nuclei compared to 3–4 nuclei, respectively), and multinucleated giant cells engulf pieces of biomaterial. Multinucleated giant cells are induced by the fusion of macrophages, a process that is dependent on the surface characteristics of the biomaterial [26]. These cells release many factors that mediate biomaterial degradation and can produce acid phosphatases and osteoclast cell markers as well [25]. This could be why these two cell types show similar TRAP positivity. Ghanaati et al. [27] proposed that a simple change in material dimensions, e.g., in the shape, size, or porosity, could also change the multinucleated giant cells response. Interestingly, multinucleated giant cells produce vascular endothelial growth factor (VEGF) [27], which may mean these cells react to foreign bodies. It may be desirable to look for biomaterials with particular shape and size characteristics that induce multinucleated giant cells to release pro-angiogenesis factors. Even though the role of these cells is unclear, we can conclude that both cell types (osteoclasts and multinucleated giant cells) contribute to the cell-based degradation of  $\beta$ -TCP. Since this process is active even 208 week after grafting, cell-based degradation is probably more important than the dissolution process in terms of removing  $\beta$ -TCP from the bone.

In one case, we observed numerous foamy histiocytes, although their role in the graft was not clear. However, their presence may have been related to the original diagnosis of nonossifying fibroma.

The quality of new bone formation and the quality of the remodeling process in the bone defect depend on both the properties of the biomaterial and on the size of the defect. In this study, we harvested samples up to 208 weeks after implantation. We evaluated biomaterial resorption and new

bone formation in cross sections of the original bone defect and compared the processes in the peripheral and central regions. In general, the peripheral regions of the original defects clearly showed new bone formation, while the central regions showed different amounts of  $\beta$ -TCP separated by sheets of hypocellular connective tissue. Similar results were shown by Hirata et al. [28]. The distance from the peripheral to the central region of the defect affects oxygen and nutrient diffusion, which may be critical in new bone formation. In trabecular bone, oxygen must generally diffuse 40 to 200  $\mu$ m between the capillary lumen and the cell membrane. This diffusion distance is critical to maintaining the balance between oxygen delivery to a site and consumption of oxygen by cells [29, 30]. In most defects seen in our clinical practice, the diffusion distance for oxygen from the edge of the defect to the center is greater than 10 mm, which is over 100-fold greater than the normal diffusion distance. In this context, limited diffusion creates a zone in the center of the defect where new bone formation is not possible and only connective tissue is present. In the seven cases presented here, these connective tissue formations were observed in the central zones. When the cavity was small, it was completely filled by bone, but when the defect was larger, it was not completely filled by bone. However, there was no necrotic tissue present, and there were some dispersed vessels in the fibrous septa. Nevertheless, this angiogenesis is too slow to enable osteogenesis. Our goal in the future is to improve the conditions in the center of the defect to better promote new bone formation. In the peripheral region of the original defect, active new bone formation, remodeling, and lamellar bone were observed despite the presence of nonresorbed biomaterial. The process of remodeling was not finished even 208 weeks after grafting, as we observed osteoblasts forming bone tissue and osteoclasts and multinuclear giant cells engulfing pieces of biomaterial.

Our observations confirmed that the physical and chemical properties of  $\beta$ -TCP make it suitable for use in bone grafts. We did not observe any adverse reactions to this material, such as necrosis or a severe inflammatory response. There was one exception, which was synovialitis of the knee due to leakage of the  $\beta$ -TCP particles into the joint space from the bone defect. Granule size and morphology, including macropore and micropore size and porosity, are generally more important for new bone ingrowth. Furthermore, Kasten et al. [31] demonstrated that the size of the pores and their interconnections are more important than the total porosity of the biomaterial. Galois and Mainard reviewed the literature to investigate what pore size was optimal for bone ingrowth. They concluded that a pore size of 80–250  $\mu$ m may be the most suitable [32]. Ghanaati et al. [27] reported that high porosity

induces faster cell and connective tissue ingrowth within the granules and concluded that the optimal porosity was about 80 % and the optimal pore size was  $<500\ \mu\text{m}$ . Materials with lower porosity only allow fine reticular connective tissue to penetrate, meaning that new bone formation foci are present adjacent to the biomaterial, separated by fine connective tissue and forming mosaic-like structures [27]. We saw something similar in our study, and the biomaterial we used had a porosity of  $35 \pm 5\%$  and an average macropore size of  $100\ \mu\text{m}$  in diameter. In all cases, histological assessment revealed similar mosaic-like patterns. Nevertheless, Lu et al. [22] reported that dissolution and cell-based phagocytic processes that occur after implantation can effectively enlarge the pore size due to degradation of the biomaterial. It is unclear whether the pores enlarge fast enough to enable better osteogenesis. Lower porosity may be responsible for lingering resorption of this biomaterial. In all cases, we saw some nonresorbed material months or even years after implantation; thus, this material can act somewhat as a place holder.

## Conclusions

Here, we performed histological examinations of biopsies from 7 patients in whom  $\beta$ -TCP was implanted to treat bone defects. We were able to observe specific histological and biochemical activity around the biomaterial. Notably, there were no histological signs of inflammatory reactions around the implanted  $\beta$ -TCP in any of the samples we examined, although mildly sclerotic bone was observed near the defect (widening of the bone trabeculae in biopsies). Osteoblasts and extracellular matrix with collagen fibrils lined the border between  $\beta$ -TCP and the host bone, and new woven and lamellar bone formation was observed as well. The presence of multinuclear giant cells engulfing the biomaterial and osteoclasts attached to the biomaterial confirmed  $\beta$ -TCP bioresorption via phagocytosis and enzymatic activity. This process was relatively slow. In fact, despite the bioresorbable nature of  $\beta$ -TCP, granules of this biomaterial were observed even 208 weeks after implantation. It was impossible to distinguish the foreign body giant cells from osteoclasts with any certainty using TRAP and CD68 immunoreactivity. However, there were differences in the level of TRAP positivity and in the structural characteristics of these cells. Depending on the size of the defect, new bone formation in the peripheral regions of the original defects was easy to see, while in the central regions,  $\beta$ -TCP granules were separated by sheets of hypocellular connective tissue. Nevertheless, the formation of new bone created mosaic-like structures in which isles of new bone were surrounded by fine fibrous tissue.

Although this report involved just 7 patients and the histological examination of just 9 biopsies, we note that there are few other published reports that provide detailed information about the healing course of human bone defects filled with synthetic ceramic material. The descriptions of these cases may thus be useful to others seeking to use  $\beta$ -TCP for this purpose.

**Acknowledgments** Authors report grants and nonfinancial support from Grant IGA MZ CR NT 13477-4 and by the Czech Republic Ministry of Health project for conceptual development of research organization 00179906, during the conduct of the study.

**Conflict of interest** None.

## References

1. De Long WG, Einhorn TA, Koval K, McKee M, Smith W, Sanders R, Watson T (2007) Bone grafts and bone graft substitutes in orthopaedic trauma surgery. *J Bone Jt Surg* 89-A: 649–659
2. De Groot K (1988) Effect of porosity and physicochemical properties on the stability, resorption, and strength of calcium phosphate ceramics. *Ann NY Acad Sci* 533:227–233
3. Ozawa M (1995) Experimental study on bone conductivity and absorbability of the pure  $\beta$ -TCP. *J Jpn Soc Biomater* 13:17–25
4. Chazono M, Tanaka T, Komaki H, Fujii K (2004) Bone formation and bioresorption after implantation of injectable  $\beta$ -tricalcium phosphate granules-hyaluronate complex in rabbit bone defects. *J Biomed Mater Res* 70-A:542–549
5. Kondo N, Ogose A, Tokunaga K, Ito T, Arai K, Kudo N, Inoue H, Irie H, Endo N (2005) Bone formation and resorption of highly purified beta-tricalcium phosphate in the rat femoral condyle. *Biomaterials* 26:5600–5608
6. Henkel KO, Bienengraber V, Lenz S, Gerber T (2005) Comparison of a new kind of calcium phosphate formula versus conventional calcium phosphate matrices in treating bone defects—a long-term investigation in pigs. *Key Eng Mater* 284–286:885–888
7. Lane JM, Yasko AW, Tomin E, Cole BJ, Waller S, Browne M, Turek T, Gross J (1999) Bone marrow and recombinant human bone morphogenetic protein-2 in osseous repair. *Clin Orthop* 361:216–227
8. Artzi Z, Weinreb M, Givol N, Rohrer MD, Nemcovsky CE, Prasad HS, Tal H (2004) Biomaterial resorption rate and healing site morphology of inorganic bovine bone and beta-tricalcium phosphate in the canine: a 24-month longitudinal histologic study and morphometric analysis. *Int J Oral Maxillofac Implants* 19:357–368
9. Gao TJ, Tuominen TK, Lindholm TS, Kommanen B, Lindholm TC (1997) Morphological and biomechanical difference in healing in segmental tibial defects implanted with biocoral or tricalcium phosphate cylinders. *Biomaterials* 18:219–223
10. Padhraig F, O'Loughlin MD, Morr S, Bogunovic L, Kim AD, Park B, Lane JM (2008) Selection and development of preclinical models in fracture-healing research. *J Bone Jt Surg* 90(Suppl 1):79–84
11. Kucera T, Urban K, Ragkou S (2012) Healing of cavitary bone defects. *Eur J Orthop Surg Traumatol* 22:123–128
12. Anker CJ, Holdridge SP, Baird B, Cohen H, Damron TA (2005) Ultraporous  $\beta$ -tricalcium phosphate is well incorporated in small cavitary defects. *Clin Orthop* 434:251–257

13. Miyauchi M, Samoto N, Muneyasu M, Shimobayashi M, Araki N, Morishita T (2005) The surgical treatment of benign bone tumors with beta-tricalcium phosphate. *Orthop Surg* 47:172–176
14. Ogose A, Kondo N, Umezu H, Hotta T, Kawashima H, Tokunaga K, Ito T, Kudo N, Hoshino M, Gu W, Endo N (2006) Histological assessment in grafts of highly purified beta-tricalcium phosphate (OSferion®) in human bones. *Biomaterials* 27:1542–1549
15. Frayssineta P, Schwartz C, Mathona D, Rouqueta N. (1999) Osteointegration of calcium phosphate ceramics in humans and animals. *MRS Proceedings/Volume* 599. doi:10.1557/PROC-599-3
16. Schwartz C, Liss P, Jacquemaire B, Lecestre P, Frayssinet P (1999) Biphasic synthetic bone substitute use in orthopaedic and trauma surgery: clinical, radiological and histological results. *J Mater Sci Mater Med* 10(12):821–825
17. Frayssinet P, Schwartz C, Beya B, Lecestre P (1999) Biology of the calcium phosphate integration in human long bones. *Eur J Orthop Surg Traumatol* 9:167–170
18. Ozawa M (1995) Experimental study on bone conductivity and absorability of the pure $\beta$ -TCP. *J Jpn Soc Biomater* 13:17–25
19. Fredericks DC, Bobst JA, Petersen EB, Nepola JV, Dennis JE, Caplan AI, Burgess AV, Overby RJ, Schulz OH (2004) Cellular interactions and bone healing responses to novel porous tricalcium phosphate bone graft material. *Orthopedics* 27(Suppl 1):167–173
20. Knaack D, Goad ME, Ailova M, Rey C, Tofighi A, Chakravarthy P, Lee D (1998) Resorbable calcium phosphate bone substitute. *J Biomed Mater Res* 43:399–409
21. Szpalski M, Gunzburg R (2002) Application of calcium phosphate-based cancellous bone void fillers in trauma surgery. *Orthopedics* 25(Suppl 5):601–609
22. Lu JX, Flautre B, Anselme K, Hardouin P, Gallur A, Descamps M, Thierry B (1999) Role of interconnections in porous bioceramics on bone recolonization in vitro and in vivo. *J Mater Sci Mater Med* 10:111–120
23. Vogel M, Voigt C, Knabe C, Radlanski RJ, Gross VM, Muller-Mai CM (2010) Development of multinuclear giant cells during degradation of Bioglass particles in rabbits. *J Biomed Mater Res A* 51:89–92
24. Abbondanzo SL, Young VL, Wei MQ, Miller FW (1999) Silicone gel-filled breast and testicular implant capsules: a histologic and immunophenotypic study. *Mod Pathol* 12:706–713
25. Kadoya Y, al-Saffar N, Kobayashi A, Revell PA (1994) The expression of osteoclast markers on foreign body giant cells. *Bone Miner* 27:85–96
26. Jones JA, Dadsetan M, Collier TO, Ebert M, Stokes KS, Ward RS (2004) Macrophage behavior on surface-modified polyurethanes. *J Biomater Sci Polym Ed* 15:567–584
27. Ghanaati S, Barbeck M, Orth C, Willershausen I, Thimm BW, Hoffmann C, Rasic A, Sader RA, Unger RE, Peters F, Kirkpatrick CJ (2010) Influence of  $\beta$ -tricalcium phosphate granule size and morphology on tissue reaction in vivo. *Acta Biomater* 6:4476–4487
28. Hirata M, Murata H, Takeshita H, Sakabe T, Tsuji Y, Kubo T (2006) Used of purified beta-tricalcium phosphate for filling defects after curettage of benign bone tumours. *Int Orthop* 30:510–513
29. Chow DC, Wenning LA, Miller WM, Papoutsakis ET (2001) Modeling pO(2) distributions in the bone marrow hematopoietic compartment. I. Krogh's model. *Biophys J* 81:675–684
30. Chow DC, Wenning LA, Miller WM, Papoutsakis ET (2001) Modeling pO(2) distributions in the bone marrow hematopoietic compartment. II. Modified Kroghian models. *Biophys J* 81:685–696
31. Kasten P, Beyen I, Niemeyer P, Luginbuhl R, Bohner M, Richter W (2008) Porosity and pore size of  $\beta$ -tricalcium phosphate scaffold can influence protein production and osteogenic differentiation of human mesenchymal stem cells: an in vitro and in vivo study. *Acta Biomater* 4:1904–1915
32. Galois L, Mainard D (2004) Bone ingrowth into two porous ceramics with different pore sizes: an experimental study. *Acta Orthop Belg* 70:598–603